Beynəlxalq Konfrans "Fizika-2005"
International Conference "Fizika-2005"
Международная Конференция "Fizika-2005"

7 - 9 İyun June Июнь 2005 №193 səhifə page стр. 729-733

Bakı, Azərbaycan Baku, Azerbaijan Баку, Азербайджан

CONSTRUCTION POTENTIALITIES OF VARIOUS TYPES OF LASERS COUPLED WITH HIGH GAIN CHARACTER AND BROAD BAND TUNABILITY IN RARE EARTH ACTIVATED THIOGALLATE COMPOUNDS

SEISHI IIDA[1,2)], ARIYUKI KATO[2)], *HIKMAT NAJAFOV[2)], CHIHARU HIDAKA[3)], TAKEO TAKIZAWA[3)]

[1)] *Sizuoka Institute of Science and Technology, Toyosawa, Fukuroi 437-8555, JAPAN*
E-mail: iida@ob.sist.ac.jp, *Tel: +81-538-45-0111, Fax: +81-538-45-0110*

[2)] *Nagaoka University of Technology, Kamitomioka, Nagaoka 940-2188, JAPAN*

[3)] *College of Humanities and Sciences, Nihon University, Tokyo 156-0045, JAPAN*
** Currently. Lewis Lab., Department of Physics, Lehigh University, Bethlehem, PA 18015-3182, USA*

Rare earth element doped thiogallate compound of $CaGa_2S_4$ is one of the most promising luminescent materials. Application possibility of Ce-doped $CaGa_2S_4$ to lasers was reported before and the possibility was also shown for stoichiometric compound of $EuGa_2S_4$. In this paper, it is shown that an alloy system of $Eu_xCa_{1-x}Ga_2S_4$ with suitably selected x value is expected to have better performance over the stoichiometric compound. Room temperature photoluminescence quantum efficiency of the alloy of $Eu_xCa_{1-x}Ga_2S_4$ was found to be nearly unity under excitation at peak wavelength of excitation spectrum (510 nm) in the x range of $0.01 \leq x \leq 0.20$, and to decrease till 30 % for stoichiometric compound $EuGa_2S_4$. This gives the maximum optical laser gain at $x \sim 0.7$, which is determined from the balance of x (Eu concentration) increase and drop of luminescence quantum efficiency with x value. Hybridization or monolithic coupling of Ce-doped $CaGa_2S_4$ and $Eu_xCa_{1-x}Ga_2S_4$, if achieved, would give wide range wavelength tunable lasers (440~540 nm:Ce, 540~600 nm:Eu), multi-color lasers and even white lasers (due to mixing of two laser colors on the chromaticity diagram). Transition probability is larger for Ce(τ_{rad} ~40 ns) than Eu(τ_{rad} ~470 ns), but this unbalance can be covered by balancing each optical gain using higher Eu concentration, taking the merit of less concentration quenching for the Eu center. High gain character of these emitting centers also would lead to possible constructions of very small lasers, surface emitting lasers, lasers with desired beam direction. Although the optical gain of ~30 cm^{-1} was confirmed to exist for $Eu_{0.2}Ca_{0.8}Ga_2S_4$ from pump-probe experiments, the pumping induced transient absorption which seems to limit the higher gain was found, and remains a problem to be studied further. Other problems and subjects to utilize full potentialities of $CaGa_2S_4$:Ce and $Eu_xCa_{1-x}Ga_2S_4$ are also described briefly.

1. INTRODUCTION

Rare earth element doped thiogallates are being studied as luminescent materials.[1-5)] Application possibility of Ce-doped $CaGa_2S_4$ to lasers was reported before[6,7)] and the possibility was also shown for stoichiometric compound of $EuGa_2S_4$.[8)] An alloy system can be formed between $CaGa_2S_4$ and $EuGa_2S_4$.[9)] In this paper, it is shown that utilization of this alloy system to laser construction has some advantage related with higher luminescence quantum efficiency compared to the stoichiometric compound. This paper explains and discusses various useful type laser constructions using $CaGa_2S_4$:Ce and the alloy system of $Eu_xCa_{1-x}Ga_2S_4$, which adds some freedom for designing a particular laser by selecting the suitable x value and gives wide potentialities, especially when hybridization or monolithic coupling of $CaGa_2S_4$:Ce and $Eu_xCa_{1-x}Ga_2S_4$ is attained.

The paper also explains pump-probe experiments for a $Eu_{0.2}Ca_{0.8}Ga_2S_4$ sample in order to examine the actual existence of optical gain in the alloy system. Although the existence of the optical gain was confirmed, excitation intensity dependence of the gain was found to show a tendency of saturation. The origin of the phenomenon is not clear at present, but this is thought to be a problem to be solved before utilizing the full merits of the system described. In order to fully utilize potentialities of these $CaGa_2S_4$:Ce and $Eu_xCa_{1-x}Ga_2S_4$, other problems and subjects to be studied are briefly described further.

2. GAIN LEVELS OF CE AND EU EMITTING CENTERS AND TUNABLE RANGE

2.1 OPTICAL GAIN CALCULATION

The emissions in discussion are related to phonon-terminated transitions. Conventional description of the laser gain for such a system can be given by McCumber's theory[10] of phonon-terminated lasers. According to this theory, gain per unit length of the stimulated emission can be calculated from the following equation.[10]

$$g(\nu) = \sigma_e \{N_+ - N_- \exp[h(\nu - \mu)/kT]\}. \quad (1)$$

Here, $\sigma_e(\nu)$ is the cross section for stimulated emission at frequency ν, N_+ and N_- are, respectively, numbers of the excited and ground state centers per cubic centimeter relevant to the transition. The $h\mu$ in eq. (1) is the excitation potential depending upon temperature, and kT is thermal energy at temperature T. At absolute zero, or at any temperature in the case where mirror-image relation holds between the emission and absorption spectra, μ coincides with the frequency of no phonon line.

$\sigma_e(\nu)$ can be expressed in terms of normalized fluorescence spectral shape function $f(\nu)$ and radiative lifetime τ with the assumption of unit quantum efficiency as follows.

$$\sigma_e(\nu) = \frac{c^2}{8\pi\nu^2 n^2 \tau} f(\nu), \quad (2)$$

where n is the refractive index of the material at frequency ν, and c is the light velocity. Actual $f(\nu)$ value at frequency ν can be calculated from experimentally measured fluorescence spectrum through the relation,

$$\int_0^\infty f(\nu)\, d\nu = 1.$$

From Eqs. (1) and (2), gain function $g(\nu)$ per unit length is obtained by substituting necessary values.

2.2 GAIN SPECTRUM OF *$CaGa_2S_4$:Ce*

The calculated gain spectrum in the case of $N_- = 0$ (ground state is completely depopulated) for $CaGa_2S_4$:Ce at room temperature is given in Fig. 1[6] in unit of N_+ in cm^{-3}. Here, the middle frequency of the region where overlapping occurs in the photoluminescence and its excitation spectra is used as μ. The value of τ is taken to be 40 ns, since the observed temperature independent value is thought to be the radiative lifetime. The value of n is taken to be 2.3,[11] ignoring its frequency dependence. The maximum gain $g_{max}(\nu_{max})$ occurs at $\nu_{max} = 6.4\text{x}10^{14}$ Hz (2.65 eV) where $f(\nu_{max}) = 1.3\text{x}10^{-14}$ sec, and the value is

$$g_{max}(\nu_{max}) = 5.2 \text{ x } 10^{-18} N_+ \text{ cm}^{-1}. \quad (3)$$

The molecular density of $CaGa_2S_4$ per cubic centimeter is $6.6\text{x}10^{21}$ cm^{-3}, since $CaGa_2S_4$ crystal contains 32 formula units in the unit cell whose lattice constants are $a=b=20.1$ Å and $c=12.1$ Å.[1] For the sample having Ce concentration of $6.6\text{x}10^{19}$ cm^{-3}(1 at.%), the maximum expected gain g_{max} becomes 340 cm^{-1} from Eq. (3). The optical gain exists in the blue to green region. Even if we consider actually observed quantum efficiency value of 30 %, the gain exceeds 100 cm^{-1} at peak of the gain spectrum.

2.3 QUANTUM EFFICIENCY AND GAIN SPECTRA OF $Eu_xCa_{1-x}Ga_2S_4$

Single crystals of $Eu_xCa_{1-x}Ga_2S_4$ ($0.01 \leq x \leq 0.4$) were grown by the Bridgeman method.[9] As reported in ref. 8), the emission spectra of Eu doped $CaGa_2S_4$ and $EuGa_2S_4$ are essentially identical except small differences of peak wavelengths and half widths. The emission spectrum of $Eu_xCa_{1-x}Ga_2S_4$ is also essentially the same to these spectra.

Figure 2 shows calculated gain spectra for several excitation levels at 77 K and 300 K using Eqs. (1) and (2) with proper values for $Eu_{0.2}Ca_{0.8}Ga_2S_4$, since a sample with this value of x=0.2 is used for gain measurements later in Section 4. The value of τ is taken to be 470 ns, since the observed low temperature value is thought to be the radiative lifetime. The value of n is taken to be 2.3, assuming the same value of $CaGa_2S_4$. In these calculations, the molecular density of $Eu_{0.2}Ca_{0.8}Ga_2S_4$ per cubic centimeter is taken to be $6.5\text{x}10^{21}$ cm^{-3}. This is the interpolated value from that of $CaGa_2S_4$ given above and $6.2\text{x}10^{21}$ cm^{-3}, that of $EuGa_2S_4$. The latter value was calculated from the fact that the crystal contains 32 formula units in the unit cell whose lattice constants are 20.45 Å, 20.71 Å and 12.22 Å.[2] The lower gain value at 300 K is due to the absorption from distribution tail of the ground state population at high temperature. In this Eu emission, the gain exists in the green to orange region.

Figure 3 shows photoluminescence quantum efficiency vs. x relation for $Eu_xCa_{1-x}Ga_2S_4$.[12] Absolute quantum efficiency measurements were done using an integration semi-sphere as described in our reports[7,8] for two samples ($EuGa_2S_4$ and $Eu_{0.01}Ca_{0.99}Ga_2S_4$). For samples with other x values, relative intensities to these two samples with corrections taking into account the real absorption at corresponding x were treated as quantum efficiency values for these samples and plotted as x dependence of quantum efficiency. Actual measurements were done using 441.6 nm laser line from a He-Cd laser. The result shown in Fig. 3 is the efficiency vs. x relation corresponding the peak of the excitation spectrum at 510 nm.[8]

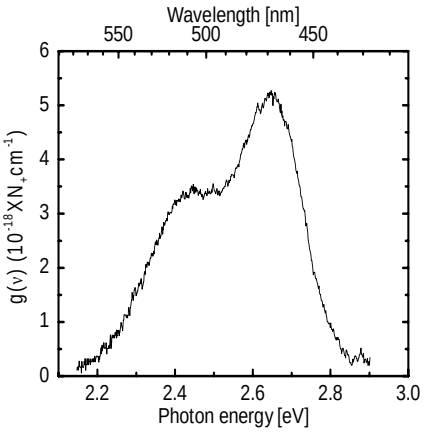

Fig. 1. Theoretically expected room temperature gain spectrum of the $CaGa_2S_4$ crystal containing Ce ions with concentration of N_+ cm^{-3} for the case of complete ground state depopulation. The spectrum is constructed using the measured fluorescence spectrum and the measured luminescence lifetime with the assumption of unit quantum efficiency.

For details, see the text.

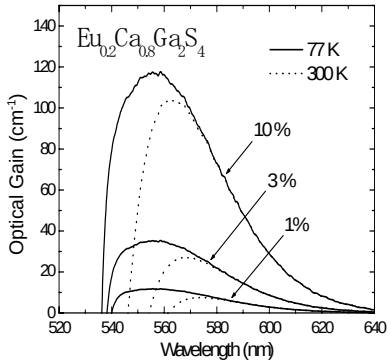

Fig.2. Calculated gain spectra of $Eu_{0.2}Ca_{0.8}Ga_2S_4$ at 77 K and 300 K based on Eqs. (1) and (2) in the text. The spectra are given for various population occupations in the excited state. These spectra are shown for 100 % quantum efficiency, since the measured room temperature quantum efficiency was nearly unity as seen in Fig. 3. For details, see the text.

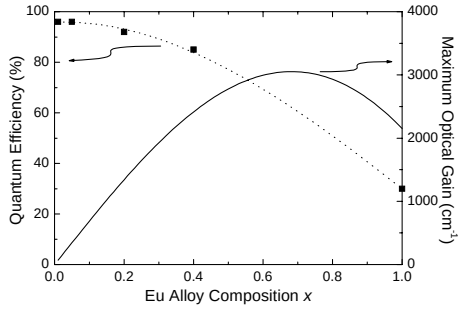

Fig. 3. x dependence of the quantum efficiency under excitation at peak wavelength of the PLE spectrum at room temperature in $Eu_xCa_{1-x}Ga_2S_4$ system, and that of calculated maximum optical gain at complete population inversion with consideration of x dependence of the quantum efficiency.

Almost unit quantum efficiency of the luminescence is seen in the range $0.01 \leq x \leq 0.20$ and the efficiency gradually decreased with x to ~30 % for x=1 ($EuGa_2S_4$) at room temperature. Figure 3 also shows x dependence of the maximum optical gain expected from Eqs. (1) and (2) with consideration of quantum efficiency corresponding to the dotted curve. The maximum optical gain as high as 3000 cm^{-1}, which is larger than that of $EuGa_2S_4$, ~2200 cm^{-1}, is expected to be obtained at x=0.7. The wide range distribution of maximum optical gain, seen in Fig. 3, gives freedom of design to select proper x values for the various types of lasers, which will be discussed in the next section.

3. VARIOUS TYPES OF POSSIBLE LASERS

3.1 LASERS WITH HIGH GAIN CHARACTER

Denoting total loss of the laser by L and the length of active region by l, threshold condition for laser oscillation at frequency ν is given by

$$g_{th}(\nu)\, l = L \,. \qquad (4)$$

Background absorption is thought to be negligible, since the energy of the emission falls fairly below the band gap energy[11] of $CaGa_2S_4$. In good lasers composed of high quality crystals, reflection loss is the major loss. Ignoring other losses, the necessary length to sustain laser oscillation is obtained from Eq. (4)

$$l = \frac{L}{g_{th}(\nu)} = \frac{1}{g_{th}(\nu)} \ln \frac{1}{R} \,.$$

From $R=(n-1)^2/(n+1)^2$ with n=2.3,[10] the length corresponding to $g_{th}(\nu)$ = 30 cm^{-1}, 50 cm^{-1}, and 100 cm^{-1} becomes 620 μm, 370 μm and 190 μm, respectively. These lengths are typical sizes of semiconductor lasers, which utilize optical processes related to band-to-band transitions. If some reduction of reflection loss is done by such means as multi-layer coating, which is usually employed, the necessary length for laser action becomes much smaller. Say for example, R=0.98 and $g_{th}(\nu)$ = 100 cm^{-1}, the length l will be ~2 μm. This length affords to make a surface emitting laser.

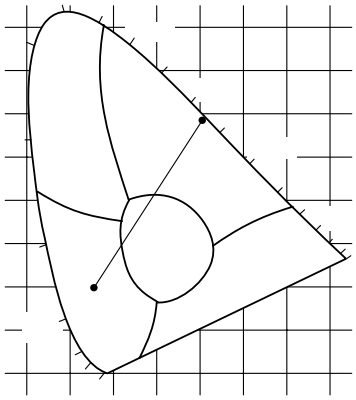

Fig. 4. Chromaticity diagram. Peak spectral positions of Ce and Eu emissions are shown in the diagram. The line connecting these positions crosses the white region.

The high gain character of the materials in discussion would also lead to constructing lasers with desired beam direction. If construction of a small sheet crystal of a polygon shape having corners of an even number is possible, the laser beam will be available for the perpendicular direction of two parallel facing side pairs with suitable position selection of pumping excitation.

3.2 LASERS WITH BROAD BAND TUNABILITY

For the case of $CaGa_2S_4$**:**Ce, the region where $g(\nu)$ value exceeds the value of 30 cm^{-1} extends from 440 nm (blue) to 550 nm (green) for N_+=6.6x10^{19} cm^{-3} (1 at.%) from Fig. 1. Even if we take an actually measured quantum efficiency value of 30 %, the region having gain values higher than 30 cm^{-1} becomes as wide as 90 nm covering blue (450 nm) to green (540 nm) region. Ce doping with concentration higher than 1 at.% gives an increase of gain value in the whole spectral region of the emission and expands the tunable wavelength region of the laser wider, as long as concentration quenching of the emission does not set in. Rather concentration-independent measured quantum efficiency values indicate that no concentration quenching occurs, at least up to 2.5 at.%.

For the case of $Eu_{0.2}Ca_{0.8}Ga_2S_4$ the gain region having gains higher than 30 cm^{-1} at 10 % population inversion at room temperature, becomes as wide as ~ 45 nm covering green (548 nm) to orange (593 nm) with assumption of

= 100 %. The assumption of 100 % quantum efficiency is reasonable, since the value of nearly 100 % was really observed as seen in Fig. 3. With larger population inversion the gain region becomes wider.

In terms of wavelength tunability of these $CaGa_2S_4$:Ce and $Eu_xCa_{1-x}Ga_2S_4$, the most interesting and useful application could be produced by combining these materials. Unification by means of hybridization or monolithic unification of these materials widens the continuous wavelength tunable range (440 nm-600 nm). Construction of multi-color lasers or even white lasers can be made from this unified material system. As can be seen from chromaticity diagram of Fig. 4, mixing of two laser colors, blue and orange, both of which lie in the tunable wavelength range can produce white color. The transition probability for the Ce center is rather high (the radiative lifetime τ_{rad} is ~ 40 ns), while that for Eu center is not so high (τ_{rad} is ~ 470 ns). There is a difference in these values by one order of magnitude or larger. However, this unbalance is not a problem for the unified material system. The optical gain is proportional to the transition probability and concentration of the emitting center. In case of Ce emitting center, no appreciable concentration quenching is seen at least up to 2.5 at.% as described before, and in the case of Eu center up to x = 0.2, no concentration quenching is seen as shown in Fig. 3. Optical gain can be balanced by using an appropriate Eu concentration (i.e., x), which is free from concentration quenching in the low x value region. Utilization of the alloy $Eu_xCa_{1-x}Ga_2S_4$ system gives useful freedom for designing the unified material system by selecting proper x value, which fits or balance with the Ce concentration.

4. PUMP-PROBE OPTICAL GAIN MEASUREMENTS OF $Eu_{0.2}Ca_{0.8}Ga_2S_4$

The experimental setup of pump-probe experiments is shown in Fig. 5. An optical parametric oscillator (Spectra Physics, MOPO-SL) pumped by the third harmonic of a Q-switched Nd:YAG laser (Spectra Physics, PRO-230-10) was used as a pump source. Wavelength, pulse duration and maximum excitation density were 500 nm, 10 ns and up to 2 MW/cm^2, respectively. This wavelength nearly corresponds to the peak of the photoluminescence excitation band.[8] The 546 nm line of a super high pressure Hg lamp (Ushio, USH-102B) was used as probe light. This wavelength lies in the photoluminescence band.

The pumping light was monitored using a photo-diode by inserting a splitting plate in the pumping pass. Emission from the front side of the sample was dispersed through a monochromator (Ritsu, MC10) and detected by a photomultiplier. Transmitted light of the probe light of the sample was dispersed by a monochromator (Jobin Yvon, HR-320) in conjunction with a photomultiplier (Toshiba, PM55). Pumping light, emission and transmitted light were recorded simultaneously by an oscilloscope (Sony Tektoronix, TDS 3054) with or without the probe light. All data were recoded using a single shot mode since shot-to-shot fluctuation of the pump light was too large to be neglected.

Figure 6(a) shows temporal variation of net intensity of the transmitted light $I(t)$ for a sample having a thickness of 23 μm. The observed transmitted light included a spontaneous emission from the back side of the sample. Therefore, net intensity of transmitted light $I(t)$ was estimated by making a correction of this emission contribution with the following equation.

$$I(t) = I^{Tr}_{Pu+\Pr}(t) - \frac{\int I^{Em}_{Pu+\Pr}(t)dt}{\int I^{Em}_{Pu}(t)dt} I^{Tr}_{Pu}(t), \quad (5)$$

where $I^{Tr}_{Pu+\Pr}(t)$ and $I^{Tr}_{Pu}(t)$ are temporal variations of the observed transmitted light with and without the probe light, respectively, and $I^{Em}_{Pu+\Pr}(t)$ and $I^{Em}_{Pu}(t)$ are those of the observed emission with and without the probe light, respectively. For comparison, temporal variation of the emission $I^{Em}_{Pu}(t)$ is shown in Fig. 6(b). The net intensity $I(t)$ shows an increase under the excitation, indicating the existence of optical gain. However, $I(t)$ turns to decrease to a negative level, indicating the existence of the pumping induced transient absorption at later stage. From the increase of $I(t)$ and the thickness of the sample, the optical gain value can be estimated. The gain value for 546 nm probe light, which is close to the peak of the photoluminescence band, was found to be ~30 cm^{-1}.

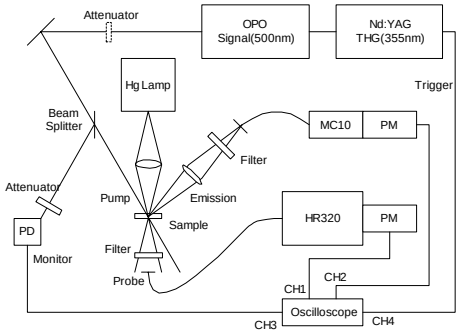

Fig. 5. Schematic diagram of arrangement of the pump-probe experiment.

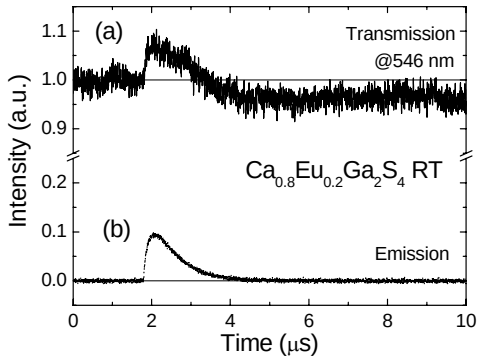

Fig. 6. Temporal variation of the transmitted light $I(t)$ at 546 nm (a) and the emission (b) for pump-probe experiment of $Ca_{1-x}Eu_xGa_2S_4$ with x=0.2.

This observed value fairly compares with theoretically calculated value based on Eqs. (1) and (2) by estimating excited Eu ion density corresponding to excitation intensity of the pumping laser and pulse duration. The estimation is given in ref. 12). However, the gain does not show further increase for higher

excitation intensity. The excitation intensity dependence of the emission intensity shows saturation behavior above 1 MW/cm^2. This saturation is probably related to the pumping induced transient absorption seen in Fig. 6(a). Even under this gain value of ~30 cm^{-1}, laser construction is thought to be possible if high quality crystals with 1 mm size are available.

5. PROBLEMS AND SUBJECTS TO BE STUDIED FURTHER

The gain saturation and pumping induced transient absorption mentioned in the previous section is a problem to be studied further for this alloy system. Whether this problem is proper to this alloy system or not has to be clarified.

For $CaGa_2S_4$**:**Ce, concentration dependence of the quantum efficiency is better to be examined for wider Ce concentration range. Further clarification of non-radiative process related to the reduction of quantum efficiency (concentration quenching) for this Ce center as well as the Eu center by means of PAS studies[13] will be useful to understand the energy transfer processes concerned and contribute to material design proper to the lasers discussed in Section 3.

A rather big target of study is to develop a proper thin film growth method compatible with Ce doping in $CaGa_2S_4$ and x controlled alloy formation of $Eu_xCa_{1-x}Ga_2S_4$. The establishment of this method would lead to full realization of the various type of lasers discussed in Section 3. Monolithic coupling of these layers could be easily done with this method, if established.

Co-doping of Eu and Ce in $CaGa_2S_4$ was reported in papers[14,15] by H. Najafov *et al.* Application possibility of co-doping was discussed and a hypothetical gain spectrum is given in Najafov's thesis.[16] Since the presence of energy transfer from Ce to Eu centers was reported, application feasibility of this co-doping to laser construction discussed above may be only in a certain limited case.

Incorporation of Ce and Eu to $SrGa_2S_4$[13] and $BaGa_2S_4$ may also be worth studying, since these materials will be similar candidates for construction of the lasers considered.

[1]. T. E. Peters and J. A. Baglio: J Electrochem. Soc. 119(1972) 230.

[2]. P. C. Donohue and J. E. Hanlon: J. Electrochem. Soc. 121(1974) 137.

[3]. S. S. Sun, R. Tuenge and M. Ling: J. Electrochem. Soc. 141(1994) 2877.

[4]. K. Tanaka, Y. Inoue, S. Okamoto and K. Kobayashi: J. Cryst. Growth 150(1995) 1211.

[5]. A. N. Georgobiani, B. G. Tagiev, O. B. Tagiev, B. M. Izzatov and R. B. Jabbarov: Cryst. Res. Technol. 32(1996) Special Issue 2 849.

[6]. S. Iida, T. Matsumoto-Aoki, T. Morita, N. Mamedov, B. G. Tagiev, F. M. Gashimzade and K. Sato: J. Appl. Phys. 39(2000) Suppl.39-1, 429.

[7]. S. Iida: IPAP Books 1(2001) 302.

[8]. S. Iida, A. Kato, M. Tanaka, H. Najafov and H. Ikuno: J. Phys. Chem. Solids 64(2003) 1815.

[9]. E. Yamagishi, C. Hidaka and T. Takizawa: presented at ICTMC-14, 2004, Denver, USA (and to be published in J. Phys. Chem. Solids).

[10]. D. E. McCumber: Phys. Rev. 134(1964) A299.

[11]. N. Mamedov, S. Iida, H. Toyota, T. Aoki-Matsumoto, A. Kato, B. Tagiev, O. Tagiev, R. Dzhabarov, N. Yamamoto and T. Shishido: Jpn. J. Appl. Phys. 39(2000) Suppl. 39-1, 287.

[12]. A. Kato, S. Iida, M. Yamazaki, E. Yamagishi, C. Hidaka and T. Takizawa: presented at ICTMC-14, 2004, Denver, USA (and to be published in J. Phys. Chem. Solids).

[13]. A. Kato, M. Yamazaki, H. Najafov, K. Iwai, A. Bayramov, C. Hidaka, T. Takizawa and S. Iida: J. Phys. Chem. Solids 64(2003) 1511.

[14]. H. Najafov, A. Kato, H. Toyota, K. Iwai, A. Bayramov and S. Iida: Jpn. J. Appl. Phys. 41(2002) 1424.

[15]. H. Najafov, A. Kato, H. Toyota, K. Iwai, A. Bayramov and S. Iida: Jpn. J. Appl. Phys. 41(2002) 2058.

[16]. H. Najafov: Doctoral Thesis(2002) (Nagaoka Univ. of Technology).